INTERNATIONAL JOURNAL OF ADAPTIVE CONTROL AND SIGNAL PROCESSING
Int. J. Adapt. Control Signal Process. 2005; **00**:1–2 *Prepared using* acsauth.cls *[Version: 2002/11/11 v1.00]*

Nonlinear Coordinated Path Following Control of Multiple Wheeled Robots with Bidirectional Communication Constraints

R. GHABCHELOO†, A. PASCOAL†, C. SILVESTRE†, and I. KAMINER‡

† *Institute for Systems and Robotics/Instituto Superior Técnico (IST), Av. Rovisco Pais 1, 1049-001 Lisboa, Portugal.*
{*reza,antonio,cjs*}*@isr.ist.utl.pt,*

‡ *Department of Mechanical and Astronautical Engineering, Naval Postgraduate School, Monterey, CA 93943, USA.*
kaminer@nps.navy.edu

SUMMARY

The paper presents a solution to the problem of steering a group of wheeled robots along given spatial paths, while holding a desired inter-vehicle formation pattern. This problem arises for example when multiple robots are required to search a given area in cooperation. The solution proposed addresses explicitly the dynamics of the cooperating robots and the constraints imposed by the topology of the inter-vehicle communications network. Lyapunov-based techniques and graph theory are brought together to yield a decentralized control structure where the information exchanged among the robots is kept at a minimum. With the set-up proposed, path following (in space) and inter-vehicle coordination (in time) are essentially decoupled. Path following for each vehicle amounts to reducing a conveniently defined error variable to zero. Vehicle coordination is achieved by adjusting the speed of each of the vehicles along its path according to information on the positions and speeds of a subset of the other vehicles, as determined by the communications topology adopted. Simulations illustrate the efficacy of the solution proposed.

KEY WORDS: Coordinated Motion Control, Graph Theory, Path following, Wheeled Robots

1. Introduction

In recent years, there has been widespread interest in the problem of coordinated motion control of fleets of autonomous vehicles. Applications include aircraft and spacecraft formation flying control (Beard *et al.*, 2001), (Giuletti *et al.*, 2000), (Pratcher *et al.*, 2001), (Queiroz

*Correspondence to: R. Ghabcheloo, reza@isr.ist.utl.pt

Contract/grant sponsor: Research supported in part by the Portuguese FCT POSI programme under framework QCA III and by project MAYA-Sub of the AdI. The first author benefited from a PhD scholarship of FCT; contract/grant number:

Received September 2005
Revised June 2006

et al., 2000), coordinated control of land robots (Desai *et al.*, 1998), (Ögren *et al.*, 2002) and control of multiple surface and underwater vehicles (Encarnação and Pascoal, 2001), (Lapierre *et al.*, 2003a), (Skjetne *et al.*, 2002), (Skjetne *et al.*, 2003), (Stilwell *et al.*, 2000). The work reported in the literature addresses a large class of topics that include, among others, leader/follower formation flying, control of the "center of mass" and radius of dispersion of swarms of vehicles, and uniform coverage of an area by a group of surveying robots.

At first inspection, the problem of coordinated motion control seems to fall within the domain of decentralized control. However, as clearly pointed out in (Fax and Murray, 2002), (Fax and Murray, 2003), it possesses several unique aspects that are at the root of new challenges to system designers. Among these, the following are worth stressing:

i) except for some cases in the area of aircraft control, the motion of one vehicle does not directly affect the motion of the other vehicles, that is, the vehicles are dynamically decoupled; the only coupling arises naturally out of the specification of the tasks that they are required to accomplish together.

ii) there are strong practical limitations to the flow of information among vehicles, which is severely restricted by the nature of the supporting communications network. In marine robotics, for example, underwater communications rely on the propagation of acoustic waves. This sets tight limits on the communication bandwidths that are achievable. Thus, as a rule, possibly no vehicle will be able to communicate with the entire formation (Fax and Murray, 2003). Furthermore, a reliable vehicle coordination scheme should exhibit some form of robustness against certain kinds of vehicle failures or loss of inter-vehicle communications.

A rigorous methodology to deal with some of the above issues has emerged from the work reported in (Fax and Murray, 2002), (Fax and Murray, 2003), which addresses explicitly the topics of information flow and cooperation control of vehicle formations simultaneously. The methodology proposed builds on an elegant framework that involves the concept of Graph Laplacian (a matrix representation of the graph associated with a given communication network). In particular, the results in (Fax and Murray, 2003) show clearly how the Graph Laplacian associated with a given inter-vehicle communication network plays a key role in assessing stability of the behavior of the vehicles in a formation. It is however important to point out in that work that: i) the dynamics of the vehicles are assumed to be linear, time-invariant, and ii) the information exchanged among vehicles is restricted to linear combinations of the vehicles' state variables.

Inspired by the progress in the field, this paper tackles a problem in coordinated vehicle control that departs slightly from mainstream work reported in the literature. Specifically, we consider the problem of *coordinated path following* where *multiple vehicles are required to follow pre-specified spatial paths while keeping a desired inter-vehicle formation pattern in time.* This mission scenario occurs naturally in underwater robotics (Pascoal *et al.*, 2000). Namely, in the operation of multiple autonomous underwater vehicles for fast acoustic coverage of the seabed. In this important case, two or more vehicles are required to fly above the seabed at the same or different depths, along geometrically similar spatial paths, and map the seabed using copies of the same suite of acoustic sensors. By requesting that the vehicles traverse identical paths so as to make the acoustic beam coverage overlap along the seabed, large areas can be covered in a short time. This imposes constraints on the inter-vehicle formation pattern. Similar scenarios can of course be envisioned for land and air vehicles.

To the best of our knowledge, previous work on coordinated path following control has essentially been restricted to the area of marine robotics. See for example (Lapierre *et*

al., 2003a), (Lapierre *et al.*, 2003b), (Skjetne *et al.*, 2002), (Skjetne *et al.*, 2003) and the references therein. However, the solutions developed so far for underactuated vehicles are restricted to two vehicles in a leader-follower type of formation and lead to complex control laws. Even in the case of fully actuated vehicles, the solutions presented do not address communication constraints explicitly. There is therefore a need to re-examine this problem to try and arrive at efficient and practical solutions.

A possible strategy is to consider similar problems for wheeled robots in the hope that the solutions derived for this simpler case may shed some light into the problem of coordinated path following for the more complex case of air and marine robots. Preliminary steps in this direction were taken in (Ghabcheloo *et al.*, 2004a), where the problem of coordinated path following of multiple wheeled robots was solved by resorting to linearization and gain scheduling techniques. The solutions obtained are conceptually simple and embody in themselves a straightforward mechanism that allows for the decoupling of path following (in space) and vehicle synchronization (in time). The price paid for the simplicity of the solutions is the lack of global results, that is, attractivity to so-called trimming paths and to a desired formation pattern can only be guaranteed locally, when the initial vehicle formation is sufficiently close to the desired one. The present paper overcomes this limitation and yields global results that allow for the consideration of arbitrary paths, formation patterns (compatible with the paths), and initial conditions. The solution adopted for coordinated path following is well rooted in Lyapunov-based theory and addresses explicitly the vehicle dynamics as well as the constraints imposed by the topology of the inter-vehicle communications network. The latter are tackled in the framework of graph theory (Godsil and Royle, 2001), which seems to be the tool par excellence to study the impact of communication topologies on the performance that can be achieved with coordination.

Once again, using this set-up, path following (in space) and inter-vehicle coordination (in time) are essentially decoupled. Path following for each vehicle amounts to reducing a conveniently defined error variable to zero. Vehicle coordination is achieved by adjusting the speed of each of the vehicles along its path according to information on the positions and speeds of a subset of the other vehicles, as determined by the communications topology adopted. No other kinematic or dynamic information is exchanged among the robots. The coordination system is simple and holds great potential to be extended and applied to the case of air and marine robots.

The paper is organized as follows. Section 2 introduces the basic notation required, describes the simplified model of a wheeled robot, and offers a novel solution to the problem of path following for a single vehicle. The main contribution of the paper is summarized in Section 3, where a strategy for multiple vehicle coordination is proposed that builds on Lyapunov and graph theory. Section 4 examines the convergence properties of the solutions of the combined path following and coordination algorithms. The proofs required are given in the Appendix. Section 5 revisits the coordination problem and provides added insight into the case where the formation pattern is time-varying. Section 6 describes the results of simulations. Finally, Section 7 contains the main conclusions and describes problems that warrant further research.

2. Path Following

This section describes a novel solution to the problem of path following for a single wheeled robot. The solution builds on and simplifies the nonlinear control law first proposed in (Soeanto *et al.*, 2003) and later re-examined in (Kaminer *et al.*, 2005). Complete details can be found in (Ghabcheloo *et al.*, 2004c).

Consider a wheeled robot of the unicycle type depicted in Figure 1, together a spatial path Γ in horizontal plane to be followed. The vehicle has two identical parallel, nondeformable rear wheels and a steering front wheel. The contact between the wheels and the ground is pure rolling and non-slipping. Each rear wheel is powered by a motor which generates a control torque. This will in turn generate a control force and a control torque applied to the vehicle. The problem of path following can now be briefly stated as follows:

Given a spatial path Γ, develop a feedback control law for the force and torque acting on a wheeled robot so that its center of mass converges asymptotically to the path while its total speed tracks a desired temporal profile.

An elegant solution to this problem was first advanced at a *kinematic* level in (Micaelli *et al.*, 1993), from which the following intuitive explanation is obtained: a path following controller should "look" at i) the distance from the vehicle to the path and ii) the angle between the vehicle's velocity vector and the tangent to the path, and reduce both to zero. This suggests that the kinematic model of the vehicle be derived with respect to a Serret-Frenet frame {T} that moves along the path, with {T} playing the role of the body-axis of a "virtual target vehicle" that must be tracked by the "real vehicle". Using this set-up, the aforementioned distance and angle become part of the coordinates of the error space where the path following control problem can be formulated and solved.

The set-up adopted in (Micaelli *et al.*, 1993) was later reformulated in (Soeanto *et al.*, 2003), leading to a feedback control law that steers the *dynamic model* of a wheeled robot with parameter uncertainty along a desired path and yields global convergence results. This is in striking contrast with the results described in (Micaelli *et al.*, 1993), where only local convergence to the path has been proven. The key enabling idea involved in the derivation of a globally convergent path following control law is to add another degree of freedom to the rate of progression of a "virtual target" to be tracked along the path, thus bypassing the singularity problems that arise in (Micaelli *et al.*, 1993) because the position of the virtual target is simply defined by the projection of the actual vehicle on that path. Formally, this is done by making the center of the Serret-Frenet frame {T} that is attached to the path evolve according to an extra "virtual" control law.

To this effect, consider Figure 1 where P is an arbitrary point on the path to be followed and Q is the origin of the body-fixed frame {B} located at the center of the mass of the vehicle. Associated with P, consider the frame Serret-Frenet {T}. The signed curvilinear abscissa of P along the path is denoted by s. Clearly, Q can be expressed either as $\mathbf{q} = (x, y)$ in the inertial reference frame {U}, or as (x_e, y_e) in {T}. Let $\mathbf{p}$ be the position of P in {U}. Further let ${}^U_T R$ and ${}^U_B R$ denote the rotation matrices from {T} to {U} and from {B} to {U} respectively, parameterized by the yaw angles ψ_T and ψ_B. Define the variables v and $r = \dot{\psi}_B$ as the linear and angular speed of the robot, respectively, calculated in {U} and expressed in {B}. From the figure, it follows that

$$\mathbf{q} = \mathbf{p} + {}^U_T R \begin{pmatrix} x_e \\ y_e \end{pmatrix}.$$

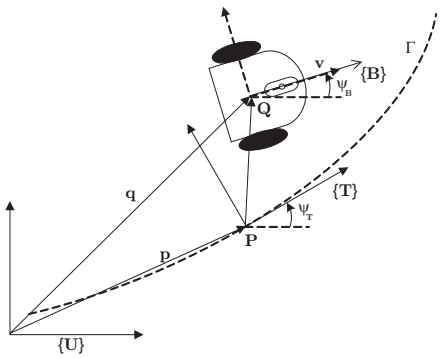

Figure 1. Frames and error variables

Taking derivatives and expressing the result in frame {U} yields

$$ {}^{U}_{B}R \begin{pmatrix} v \\ 0 \end{pmatrix} = {}^{U}_{T}R \begin{pmatrix} \dot{s} \\ 0 \end{pmatrix} + {}^{U}_{T}\dot{R} \begin{pmatrix} x_e \\ y_e \end{pmatrix} + {}^{U}_{T}R \begin{pmatrix} \dot{x}_e \\ \dot{y}_e \end{pmatrix} $$

From the above expression, simple calculations lead to the kinematics of the robot in the (x_e, y_e) coordinates as

$$ \text{Kinematics} \begin{cases} \dot{x}_e &= (y_e c_c(s) - 1)\dot{s} + v\cos\psi_e \\ \dot{y}_e &= -x_e c_c(s)\dot{s} + v\sin\psi_e \\ \dot{\psi}_e &= r - c_c(s)\dot{s}. \end{cases} \tag{1} $$

where $\psi_e = \psi_B - \psi_T$ and $c_c(s)$ is the path curvature at P determined by s, that is, $\dot{\psi}_T = c_c(s)\dot{s}$. Notice how the kinematics are driven by v, r and also by the term $\dot{s}$ that plays the role of an extra control signal.

Under the usual simplifying assumptions, the dynamics of the wheeled robot can be written as

$$ \text{Dynamics} \begin{cases} \dot{v} = F/m \\ \dot{r} = N/I \end{cases} \tag{2} $$

where m denotes the mass of the robot, I is the moment of inertia about the vertical body-axis, and F and N denote the total force and torque, respectively, applied to the vehicle. We assume without loss of generality that $m = I = 1$ in the appropriate units. With this set-up, the problem of path following can be mathematically formulated as follows:

> **Problem 1 [Path Following].** Given a spatial path Γ and a desired speed path profile $v_d(t)$ for the vehicle speed v, derive feedback control laws for F, N and $\dot{s}$ to drive x_e, y_e, ψ_e, and $v - v_d$ asymptotically to 0.

Driving the speed v to the desired speed is trivial to do with the simple control law $F = \dot{v}_d - k_0(v - v_d)$, which makes the error $v - v_d$ decay exponentially to zero. Controlling v is therefore decoupled from the control of the other variables, and all that remains is to find suitable control laws for N and for $\dot{s}$ to drive x_e, y_e, ψ_e to zero, no matter what the evolution of $v(t)$ is. The only technical assumptions required are that the path be sufficiently smooth and that $\lim_{t\to\infty} v(t) \neq 0$.

Proposition 1 [Path Following]. Let Γ be a path to be followed by a wheeled robot. Further let the kinematic and dynamic equations of motion of the robot be given by (1) and (2), respectively. Assume $v(t)$ is uniformly continuous and $\lim_{t\to\infty} v(t) \neq 0$. Define

$$\begin{aligned} \sigma = \sigma(y_e) &= -\text{sign}(v)\sin^{-1}\tfrac{k_2 y_e}{|y_e|+\epsilon_0} \\ \delta = \delta(\psi_e,\sigma) &= \begin{cases} 1 & \text{if } \psi_e = \sigma \\ \frac{\sin\psi_e - \sin\sigma}{\psi_e - \sigma} & \text{otherwise} \end{cases} \\ \phi &= c_c\dot{s} + \dot{\sigma} - k_1(\psi_e - \sigma) - v y_e \delta \end{aligned} \tag{3}$$

for some $k_1 > 0$, $0 < k_2 \leq 1$ and $\epsilon_0 > 0$. Let the control laws for N and $\dot{s}$ be given by

$$N = \dot{\phi} - k_4(r - \phi) - (\psi_e - \sigma) \tag{4}$$

$$\dot{s} = v\cos\psi_e + k_3 x_e \tag{5}$$

for some $k_3, k_4 > 0$. Then, $(x_e, y_e, \psi_e) = (0, 0, 0)$ is a globally asymptotically stable equilibrium point.

Proof. See the Appendix.

At this point, it is important to give some intuition for the control law proposed. As will be seen later, the proof starts with the Lyapunov function $V = \frac{1}{2}x_e^2 + \frac{1}{2}y_e^2 + \frac{1}{2}(\psi_e - \sigma)^2 + \frac{1}{2}(r-\phi)^2$. The first two terms capture the distance between the robot and the virtual target, which must be reduced to 0. The third term aims to shape the approach angle of the robot to the path as a function of the distance y_e, by forcing it to follow a desired orientation profile embodied in the function σ. See (Micaelli *et al.*, 1993) where this strategy was first introduced. Finally, the fourth term is a by-product of the backstepping technique that lies at the root of the proof and aims to force the actual rate of rotation r of the robot to track a desired profile that is determined at the kinematic level. The control laws for torque N and virtual target speed $\dot{s}$ follow from Lyapunov theory. Under the above conditions, $\dot{s}$ tends to v, that is, the speed of the virtual target approaches v asymptotically. Furthermore, r approaches $c_c\dot{s} = c_c v$ as t increases.

3. Coordination

Equipped with the results obtained in the previous section, we now consider the problem of coordinated path following control that is the main contribution of the present paper. In the most general set-up, one is given a set of $n \geq 2$ wheeled robots and a set of n spatial paths Γ_k; $k = 1, 2, ..., n$ and require that robot k follow path Γ_k. We further require that the vehicles move along the paths in such a way as to maintain a desired formation pattern compatible with those paths. The speeds at which the robots are required to travel can be imposed in a number of ways; for example, by nominating one of the robots as a formation leader, assigning it a desired speed, and having the other robots adjust their speeds accordingly. Figures 2 and 3 show the simple cases where 3 vehicles are required to follow the straight paths or circumferences $\Gamma_i; i = 1, 2, 3$ while keeping a desired "triangle" or "in-line" formation pattern.

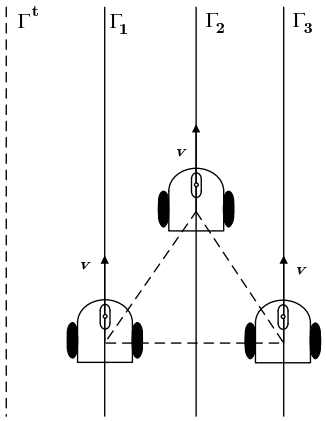

Figure 2. Coordination: triangle formation

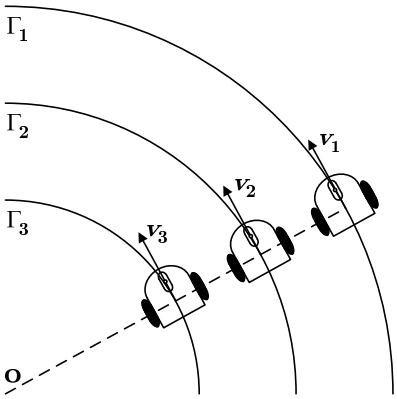

Figure 3. Coordination: in-line formation

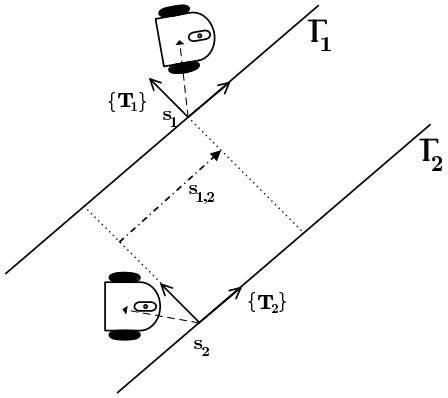

Figure 4. Along-path distances: straight lines

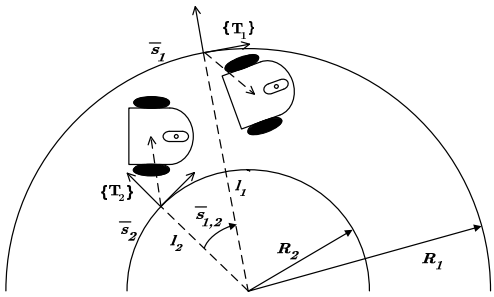

Figure 5. Along-path distances: circumferences

In the simplest case, the paths Γ_i may be obtained as simple parallel translations of a "template" path Γ^t (Figure 2). A set of paths can also be obtained by considering the case of scaled circumferences with a common center and different radii R_i (Figure 3).

Assuming that separate path following controllers have been implemented for each robot, it now remains to coordinate (that is, synchronize) them in time so as to achieve a desired formation pattern. As will become clear, this will be achieved by adjusting the speeds of the robots as functions of the "along-path" distances among them. To better grasp the key ideas involved in the computation of these distances, consider for example the case of in-line formations maneuvering along parallel translations of straight lines. For each robot i, let s_i denote the signed curvilinear abscissa of the origin of the corresponding Serret-Frenet frame $\{\mathrm{T}_i\}$ being tracked, as introduced in the previous section. Since each vehicle body-frame $\{\mathrm{B}_i\}$ tends asymptotically to $\{\mathrm{T}_i\}$, it follows that the vehicles are (asymptotically) synchronized if

$$s_{i,j}(t) := s_i(t) - s_j(t) \to 0, t \to \infty; i = 1, .., n; i < j \leq n. \tag{6}$$

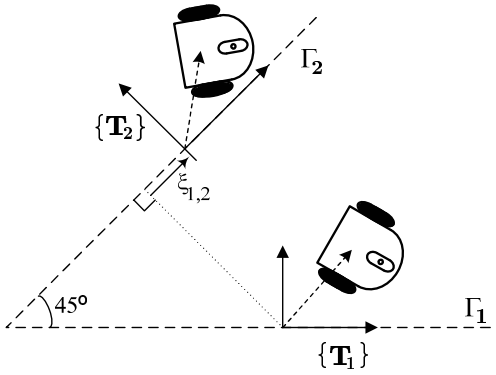

Figure 6. A general coordination scheme

This shows that in the case of translated straight lines $s_{i,j}$ is a good measure of the along-path distances among the robots. Similarly, in the case of scaled circumferences an appropriate measure of the distances among the robots is

$$\bar{s}_{i,j} := \bar{s}_i - \bar{s}_j; i = 1, .., n; i < j \leq n \tag{7}$$

where $\bar{s}_i = s_i/R_i$. See Figures 4 and 5.

Notice how the definition of $\bar{s}_{i,j}$ relies on a normalization of the lengths of the circumferences involved and is equivalent to computing the angle between vectors l_i and l_j directed from the center of the circumferences to origin of the Serret-Frenet frames $\{\mathrm{T}_i\}$ and $\{\mathrm{T}_j\}$, respectively. In both cases, we say that the vehicles are coordinated if the corresponding along path distance is zero, that is, $s_i - s_j = 0$ or $\bar{s}_i - \bar{s}_j = 0$. The extension of these concepts to a more general setting requires that each path Γ_i be parameterized in terms of a parameter ξ_i that is not necessarily the arc length along the path. An adequate choice of the parameterization will allow for the conclusion that the vehicles are synchronized iff $\xi_i = \xi_j$ for all i, j. For example, in the case of two robots following two circumferences with radii R_1 and R_2 while keeping an in-line formation pattern, $\xi_i = s_i/R_i; i = 1, 2$. This seemingly trivial idea allows for the study of more elaborate formation patterns. As an example, consider the problem depicted in Figure 6 where vehicles 1 and 2 must follow paths Γ_1 and Γ_2 while maintaining vehicle 2 "to-the-left-and-behind" vehicle 1, that is, along straight lines that make an angle of 135 degrees with the positive direction of path Γ_1. Let $\xi_1 = s_1$ and $\xi_2 = s_2\sqrt{2}$. It is clear the vehicles are synchronized if $\xi_1 - \xi_2 = 0$. Since the objective of the coordination is to synchronize ξ_i's, we sometimes refer to them as *coordination states*.

The above considerations motivate the mathematical development that follows. We start by computing the coordination error dynamics, after which a decentralized feedback control law is derived to drive the coordination error to zero asymptotically. In the analysis, graph theory - as the mathematical machinery par excellence to deal with inter-vehicle communication constraints - will play a key role.

3.1. Coordination error dynamics

As before, we let the path Γ_i be parameterized by ξ_i and denote by $s_i = s_i(\xi_i); i = 1, 2, ..., n$ the corresponding arc length. We define $R_i(\xi_i) = \partial s_i/\partial \xi_i$ and assume that $R_i(\xi_i)$ is positive and uniformly bounded for all ξ_i. In particular, s_i is a monotonically increasing function of ξ_i. We further assume that all $R_i(\xi_i)$ is bounded away from 0 and that $\partial R_i/\partial \xi_i$ is uniformly bounded. The symbol $R_i(.)$ is motivated by the nomenclature adopted before for the case of paths that are nested arcs of circumferences. Using equation (5), it is straightforward to show that the evolution of ξ_i is given by

$$\dot{\xi}_i = \frac{1}{R_i(\xi_i)}(v_i \cos\psi_{ei} + k_{3i} x_{ei}), \tag{8}$$

which can be re-written as

$$\dot{\xi}_i = \frac{1}{R_i(\xi_i)} v_i + d_i, \tag{9}$$

where

$$d_i = \frac{1}{R_i(\xi_i)}\,[(\cos\psi_{ei} - 1)v_i + k_{3i} x_{ei}]. \tag{10}$$

Notice from the previous section that $d_i \to 0$ asymptotically as $t \to \infty$, if v_i is bounded. In the Appendix, in the proof of Proposition 3, it will be shown that this assumption is met. Suppose one vehicle, henceforth referred to as vehicle $\mathcal{L}$, is elected as "leader" and let the corresponding path $\Gamma_{\mathcal{L}}$ be parameterized by its length, that is, $\xi_{\mathcal{L}} = s_{\mathcal{L}}$. In this case, $R_{\mathcal{L}}(\xi_{\mathcal{L}}) = 1$. It is important to point out that $\mathcal{L}$ can always be taken as a "virtual" vehicle that is added to the set of "real" vehicles as an expedient to simplify the coordination strategy. Let $v_{\mathcal{L}} = v_{\mathcal{L}}(t)$ be a desired speed profile assigned to the leader in advance, that is $\dot{\xi}_{\mathcal{L}} = v_{\mathcal{L}}$, and known to all the other vehicles. Notice now that in the ideal steady situation where the vehicles move along their respective paths while keeping the desired formation, we have $\xi_i - \xi_{\mathcal{L}} = 0$ and therefore $\dot{\xi}_i = v_{\mathcal{L}}$ for all $i = 1, .., n$. Thus, $v_{\mathcal{L}}$ becomes the desired speed of each of the vehicles, *expressed in ξ_i coordinates*. As such, *one can proceed without having to resort to the concept of an actual or virtual leader vehicle, thus making the coordination scheme truly distributed*.

From (9), making $d_i = 0$, it follows that the desired inertial velocities of vehicles $1 \le i \le n$ equal $R_i(\xi_i)v_{\mathcal{L}}(t)$. This suggests the introduction of the speed-tracking error vector

$$\eta_i = v_i - R_i(\xi_i)v_{\mathcal{L}}, \;\; 1 \le i \le n. \tag{11}$$

Taking into account the vehicle dynamics yields

$$\dot{\eta}_i = u_i = F_i - \frac{d}{dt}\left(R_i(\xi_i)v_{\mathcal{L}}\right). \tag{12}$$

Using (9), it is also easy to compute the dynamics of the origin of each Serret-Ferret frame $\{\mathrm{T}_i\}$ as

$$\dot{\xi}_i \;\; = \;\; \tfrac{1}{R_i}\eta_i + v_{\mathcal{L}} + d_i. \tag{13}$$

To write the above dynamic equations in vector form, define $\eta = [\eta_i]_{n\times 1}$, $\xi = [\xi_i]_{n\times 1}$, $u = [u_i]_{n\times 1}$, $d = [d_i]_{n\times 1}$ and $C = C(\xi) = \mathrm{diag}[1/R_i(\xi_i)]_{n\times n}$ to obtain

$$\begin{array}{rcl} \dot{\eta} & = & u \\ \dot{\xi} & = & C\eta + v_{\mathcal{L}}\mathbf{1} + d \end{array} \tag{14}$$

where $\mathbf{1} = [1]_{n\times 1}$. In the above, $||d|| \to 0$ asymptotically as $t \to \infty$ and matrix C is positive definite and bounded, that is,

$$0 < c_1 I \leq C(\xi(t)) \leq c_2 I \tag{15}$$

for all t, where c_1 and c_2 are positive scalars and I the identity matrix. Notice that C is allowed to be (state-driven) time-varying, thus allowing for more complex formation patterns than those in the motivating examples of the previous section.

The objective is to derive a control strategy for u to make $\xi_1 = ... = \xi_n$ or, equivalently, $(\xi_i - \xi_j) = 0$ for all i, j. At this point, however, two extremely important control design constraints must be taken into consideration. The first type of constraints is imposed by the topology of the inter-vehicle communications network (that is, by the types of links available for communication). The second type of constraints arises from the need to drastically reduce the amount of information that is exchanged over the communications network. In this paper, it will be assumed that the vehicles only exchange information on their positions and speeds. The case where only position information is exchanged leads to more complex coordination control laws and will not be examined here.

A possible control law is of the form

$$u_i = u_i(\eta_i, \xi_i, \eta_j, \xi_j : j \in J_i) \tag{16}$$

where J_i is the index set (of the neighbors) that determines what coordination states ξ_j and speed-tracking errors η_j; $j \neq i$ are transmitted to vehicle i. With this control law, each vehicle i requires only access to its own speed-tracking error and coordination state and to some or all of the coordination states and speed-tracking errors of the remaining vehicles, as defined by the index set J_i. Throughout the paper, we assume that the *communication links are bidirectional*, that is, if vehicle i sends information to j, then j also sends information to i. Formally, $i \in J_j \Leftrightarrow j \in J_i$. Clearly, the index sets capture the type of communication structure that is available for vehicle coordination. This suggests that the vehicles and the data links among them be viewed as a graph where the vehicles and the data links play the role of vertices of the graph and edges connecting those vertices, respectively. It is thus natural that the machinery of graph theory be brought to bear on the definition of the problem under study.

3.2. Graphs. Graph-induced coordination error

We summarize below some key concepts and results of graph theory that are relevant to the paper. See for example (Biggs, 1996), (Godsil and Royle, 2001), and (Balakrishnan and Ranganathan, 2000), and the references therein.

3.2.1. Basic Concepts and Results

An *undirected graph* or simply a graph $\mathcal{G}(\mathcal{V}, \mathcal{E})$ (abbv. $\mathcal{G}$) consists of a set of *vertices* $V_i \in \mathcal{V}(\mathcal{G})$ and a set of *edges* $\mathcal{E}(\mathcal{G})$, where an edge $\{V_i, V_j\}$ is an unordered pair of distinct vertices V_i and V_j in $\mathcal{V}(\mathcal{G})$. A *simple graph* is a graph with no edges from one vertex to itself. In this paper we only consider simple graphs, and will refer to them simply as graphs. As stated before, in the present work the vertices and the edges of a graph represent the vehicles and the data links among the vehicles, respectively. If $\{V_i, V_j\} \in \mathcal{E}(\mathcal{G})$, then we say that V_i and V_j are *adjacent* or *neighbors*. A *path* of length N from V_i to V_j in a graph is a sequence of $N + 1$ distinct vertices starting with V_i and ending with V_j, such that two consecutive vertices are adjacent.

The graph $\mathcal{G}$ is said to be *connected* if two arbitrary vertices V_i and V_j can be joined by a path of arbitrary length.

The assumption that all communication links are bidirectional seems to imply that no specific orientations should be assigned to the edges of the underlying coordination graph. This is true from a pure communications standpoint. However, the fact that we wish the coordination control law to reflect the topology of the communication network requires that we take a different approach to the problem at hand. To see this, let $\mathcal{G}$ be the undirected graph that captures the bidirectional communication network. Then, $\mathcal{G}$ has n vertices (as many as the vehicles). Associate to each vertex i the respective coordination state ξ_i. As discussed before, it is the objective of the coordination system to drive the errors $(\xi_i - \xi_j)$ to 0 for all i, j. This suggests that the coordination control law have access to all or some of the errors thus defined, as determined by the communication network. Suppose vertices i and j can communicate with each other. Then, it is natural that the overall coordination error vector (to be reduced to 0) include all allowable $\xi_i - \xi_j$ or a combination thereof. The important fact is that the $+$ and $-$ signs involved in the computation of the error components naturally introduce an orientation in the coordination graph from vertex j to vertex i. To make this circle of ideas formal we recall the definition of orientation of a graph and related concepts.

An *orientation* of a graph $\mathcal{G}$ is the assignment of a direction to each edge of that graph. To do this, select for each edge $\{V_i, V_j\}$ in $\mathcal{E}(\mathcal{G})$ one of the V_i, V_j to be the head of the edge and the other the tail, and view the edge oriented from its tail to its head. After this operation, the elements of $\mathcal{E}(\mathcal{G})$ become ordered pairs (V_i, V_j), henceforth known as *arcs*. See Figure 7 for the case of a graph with three vertices. Formally, an orientation of $\mathcal{G}$ can be defined as a function σ from the arcs of $\mathcal{G}$ to $\{-1, 1\}$ such that if (V_i, V_j) is an arc then $\sigma(V_i, V_j) = -\sigma(V_j, V_i)$. If $\sigma(V_i, V_j) = 1$, then we regard the arc (V_i, V_j) as oriented from tail V_i to head V_j. An oriented graph is a graph with a particular orientation denoted $\mathcal{G}^\sigma$. The *incidence matrix* M of $\mathcal{G}^\sigma$ is the $\{0, \pm 1\}$-matrix with rows and columns indexed by the vertices and the arcs of $\mathcal{G}^\sigma$, respectively. If $\mathcal{G}^\sigma$ has n vertices and ϵ arcs, M is of order $n \times \epsilon$ and its kl-entries are

$$m_{kl} = \begin{cases} +1, & \text{if } V_k \text{ is the head of arc } l \\ -1, & \text{if } V_k \text{ is the tail of arc } l \\ 0, & \text{otherwise} \end{cases} \tag{17}$$

where an arbitrary numbering of the arcs is assumed. Note that each column of M contains only two non-zero entries, $+1$ and -1, representing the head and the tail of the incident arc. The following result plays a key role in the development that follows.

> **Lemma 1.** (Godsil and Royle, 2001) *Let $\mathcal{G}$ be a graph with ϵ edges and n vertices. Let M be the incidence matrix of $\mathcal{G}^\sigma$ with an arbitrary orientation σ. If $\mathcal{G}$ is connected, then $\epsilon \geq n - 1$,* $\mathrm{Rank} M^T = n - 1$, *and* $\mathrm{Kern} M^T = \mathbf{1}$.

We close this short introduction to graph theory by introducing the concept of *Laplacian* of an undirected graph (Biggs, 1996). Let $\mathcal{G}$ be an *undirected graph* with n vertices and assign an arbitrary orientation to it. Consider the corresponding incidence matrix M. The *Laplacian* L of $\mathcal{G}$ is the symmetric, positive semi-definite square matrix $L = MM^T$ of order $n \times n$. This definition of Laplacian is equivalent to the more used one of $L = D - A$, where D and A denote the degree matrix and the adjacency matrix of $\mathcal{G}$, respectively. By construction, L is *independent* of the particular orientation assigned to an undirected graph $\mathcal{G}$. Furthermore,

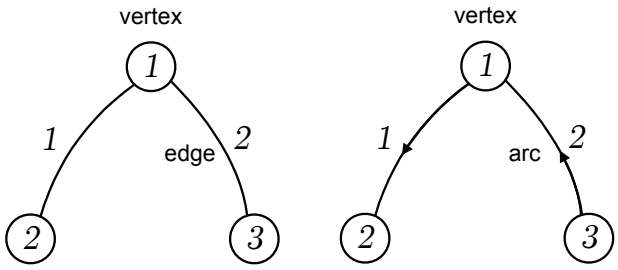

Figure 7. Left: An undirected graph. Right: The undirected graph with an associated orientation

all eigenvalues of L are non-negative, and $L\mathbf{1} = \mathbf{0}$. If $\mathcal{G}$ is connected, Rank$L = n - 1$ and consequently L has a single eigenvalue at zero with corresponding right eigenvector $\mathbf{1}$. Furthermore, the diagonal elements of the Laplacian matrix of a connected graph are positive and the off diagonal terms are non-positive. The following example illustrates some of these properties.

Example 1. Consider the graph $\mathcal{G}$ of Figure 7 with the orientation inherited from the directions assigned to its edges. Then,

$$M = \begin{pmatrix} -1 & 1 \\ 1 & 0 \\ 0 & -1 \end{pmatrix} \text{ and } L = \begin{pmatrix} 2 & -1 & -1 \\ -1 & 1 & 0 \\ -1 & 0 & 1 \end{pmatrix}.$$

Given any arbitrary vector ζ,

$$L\zeta = \begin{pmatrix} \zeta_1 - \zeta_2 + \zeta_1 - \zeta_3 \\ \zeta_2 - \zeta_1 \\ \zeta_3 - \zeta_1 \end{pmatrix}.$$

Moreover if $y = L\zeta$, then the i'th element of y is

$$y_i = \sum_{j \in J_i} (\zeta_i - \zeta_j),$$

that is, y_i is a linear combination of the terms $(\zeta_i - \zeta_j)$, where j spans the set J_i of vehicles that i communicates with. This seemingly trivial point plays a key role in the computation of a decentralized coordination control law that takes into consideration the a priori existing communication constraints, as will become clear later.

In preparation for the next section we now recall a set of more advanced results in graph theory.

3.2.2. Spanning tree of a graph.

A *subgraph* of a graph $\mathcal{G}$ is a graph $\mathcal{G}_1$ such that $\mathcal{V}(\mathcal{G}_1) \subseteq \mathcal{V}(\mathcal{G})$ and $\mathcal{E}(\mathcal{G}_1) \subseteq \mathcal{E}(\mathcal{G})$. If $\mathcal{V}(\mathcal{G}_1) = \mathcal{V}(\mathcal{G})$, we call $\mathcal{G}_1$ a *spanning subgraph* of $\mathcal{G}$. A *cycle* is a close path (that is, a path from vertex V_i to itself) in which the intermediate edges are all distinct. A connected graph

without cycles is defined as a *tree*. The following two lemmas are borrowed from (Balakrishnan and Ranganathan, 2000).

Lemma 2. *Every connected graph contains a spanning tree.*

Lemma 3. *The number of edges in a tree with n vertices is $n-1$. Conversely, a connected graph with n vertices and $n-1$ edges is a tree.*

These results are now exploited to give further insight into the structure of a connected graph $\mathcal{G}$ with n vertices and ϵ edges. Since $\mathcal{G}$ is connected, $\epsilon \geq n-1$. We analyze the cases $\epsilon \geq n$ and $\epsilon = n-1$ separately.

Suppose $\epsilon \geq n$ and choose a spanning tree $\mathcal{T}$ in $\mathcal{G}$, which is known to exist because of Lemma 2. Lemma 3 ensures that the spanning tree has $n-1$ edges. Index the edges of $\mathcal{G}$ that are in $\mathcal{T}$ from 1 to $n-1$ and the remaining edges from n to ϵ. Associate now an arbitrary orientation σ to graph $\mathcal{G}$ and compute the corresponding incidence matrix M of $\mathcal{G}^\sigma$. Finally, partition M as $M = [M_1, M_2]$, where $M_1 \in \mathbb{R}^{n \times n-1}$ becomes the incidence matrix of $\mathcal{T}^\sigma$ with the orientation inherited from $\mathcal{G}^\sigma$.

Since $\mathcal{T}$ is connected, $\mathrm{Rank} M_1 = n-1$ and $M_1^T M_1$ is invertible. Define $U = M_2^T M_1 (M_1^T M_1)^{-1}$. Then, M_2 and M_1 are related through the expression $M_2^T = U M_1^T$. Close inspection of U shows that it is a matrix with entries in the set $\{0, \pm 1\}$. This is a simple consequence of the following two facts: i) the columns of M_1 are linearly independent and each column of M_2 is a linear combination of the columns of M_1, and ii) given an arbitrary column of M_2, the coefficients of its expansion in terms of the columns of M_1 are $+1$ or -1. To see this, consider an arbitrary edge $i \geq n$ (corresponding to column $j = i - n + 1$ of M_2), joining vertices V_k and V_l. $\mathcal{T}$ is connected, and therefore there exists a path Γ from V_k to V_l entirely contained in $\mathcal{T}$. Because the edges in this path correspond to a subset of the columns $1, ..., n-1$ of matrix M_1 and each edge has an assigned orientation, the results follow. In view of the above, the Laplacian of $\mathcal{G}$ admits the representation

$$L = M M^T = (M_1 Y)(M_1 Y)^T \tag{18}$$

with

$$Y^2 = I + U^T U; Y > 0. \tag{19}$$

Consider now the case where $\epsilon = n-1$ edges (that is, $\mathcal{G}$ is already a tree). The above equalities apply with $U = 0$ and $Y = I$. Furthermore, M_2 is obviously null.

Example 2. Consider the connected graph $\mathcal{G}$ that is obtained by adding to that of Figure 7 an extra edge $\{V_2, V_3\}$ with orientation $\sigma(V_2, V_3) = 1$. The resulting graph is not a tree. However, it admits an obvious spanning tree for which

$$M_1 = \begin{pmatrix} -1 & 1 \\ 1 & 0 \\ 0 & -1 \end{pmatrix}, M_2 = \begin{pmatrix} 0 \\ -1 \\ 1 \end{pmatrix}, U^T = \begin{pmatrix} -1 \\ -1 \end{pmatrix}, \text{ and } Y^2 = \begin{pmatrix} 2 & 1 \\ 1 & 2 \end{pmatrix}.$$

3.3. Coordination. Problem formulation and solutions

We now state the coordination problem that is the main focus of this section. First, however we comment on the type of communication constraints considered in the paper. It is assumed that: i) the *communications are bidirectional* and ii) the *communications graph is connected*. Notice that if assumption (ii) is not verified, then there are two or more clusters of vehicles and no information is exchanged among the clusters. Clearly, in this situation no coordination is possible.

Problem 2 [Coordination]. *Consider the coordination system with dynamics (14) and assume that d tends asymptotically to $\mathbf{0}$. Further assume that each of the n vehicles has access to its own state and exchanges information on its path parameter (coordination state) ξ_i and speed-tracking error η_i with some or all of the other vehicles. Let $\mathcal{G}$ be a graph with n vertices and ϵ edges, where the presence of an edge between vertex i and j signifies that vehicle i and j communicate through a bidirectional link. Determine a feedback control law for u such that $\lim_{t\to\infty}\eta = \mathbf{0}$ and $\lim_{t\to\infty}(\xi_i - \xi_j) = 0$ for all $i, j = 1, .., n$.*

Remark 1. The assumption that d tends asymptotically to $\mathbf{0}$ as $t \to \infty$ will be justified in Section 4, which contains the analysis of the dynamic behavior of the combined path following and coordination systems.

The next proposition offers a solution to the coordination problem, under the basic assumption that the communications graph $\mathcal{G}$ is connected.

Proposition 2 [Solution to the coordination problem]. *Consider the coordination problem described before and assume that the communications graph $\mathcal{G}$ is connected and the disturbance-like term d is zero. Let $L = MM^T$ be the Laplacian of $\mathcal{G}$ where M is the incidence matrix that is obtained with an arbitrary orientation on graph $\mathcal{G}$. Further let $A = \mathrm{diag}[a_i]_{n\times n}$ and $B = \mathrm{diag}[b_i]_{n\times n}$ be arbitrary positive definite diagonal matrices. Then, the control law*

$$u = -(A^{-1}L + A)C\eta - B\,\mathrm{sat}(\eta + A^{-1}L\xi), \tag{20}$$

where sat *is the saturation function*

$$\mathrm{sat}(x) = \begin{cases} x_m & x > x_m \\ x & |x| \le x_m \\ -x_m & x < -x_m \end{cases} \tag{21}$$

with $x_m > 0$ arbitrary, solves the coordination problem. Namely, the control law meets the communication constraints and the origin is a uniformly globally asymptotically stable (UGAS) equilibrium point of the coordination closed-loop subsystem.

Proof. See the Appendix where it will be shown that the solution derived yields a decentralized control law that meets the communication constraints. The case $d \neq \mathbf{0}$ is treated in Section 4 where we study the path-following and coordination interconnection.

We now examine the form of the control law adopted, which can be written as

$$u_i = -\frac{a_i}{R_i}\eta_i - \frac{1}{a_i}\sum_{j\in J_i}(\frac{1}{R_i}\eta_i - \frac{1}{R_j}\eta_j) - b_i\,\mathrm{sat}(\eta_i + \frac{1}{a_i}\sum_{j\in J_i}(\xi_i - \xi_j)). \tag{22}$$

We recall that J_i denotes the set of vehicles (vertices in the graph) that communicate with vehicle i. Notice how the control input of vehicle i is a function of its own speed-tracking error and coordination state as well as of the coordination states and speed-tracking errors of the other vehicles included in the index set J_i. Clearly, the control law is decentralized and meets the constraints imposed by the communications network, as required.

Matrices A and B play the role of tuning knobs aimed at shaping the behavior of the coordination system. Notice that the coordination vector ξ appears inside the s*at* function. From the form of control law, it is clear that the s*at* function affords the system designer an extra degree of freedom because as x_m increases, the control activity u becomes more "responsive" to vector ξ (intuitively, as x_m increases, the coordination dynamics become "faster"). Interestingly enough, the introduction of the s*at* function allows for a simple proof that $v(t)$ remains bounded when the path following and coordination systems are put together.

4. Path Following and Coordination Interconnection

This section examines the behavior of the *coordinated path following system* that results from putting together the path following control and the coordination control systems presented in the previous sections. In particular, we show that the trajectories of *the relevant state variables tend asymptotically to* 0 if the positive definite matrix A satisfies an additional technical condition, as shown below. For simplicity of exposition, we make $A = aI, a > 0$.

Proposition 3 [Coordinated Path Following]. *Consider the closed-loop system consisting of the Path Following (P.F.) and Coordination Control (C.C.) subsystems of Propositions 1 and 2, respectively depicted in Figure 8. Let* $X_{pi} = (x_{ei}, y_{ei}, \psi_{ei})^T$; $1 \le i \le n$ *denote the state of the path following subsystem of each vehicle. Further let* $X_c = (\eta^T, \theta^T)^T$ *be the relevant state of the coordination subsystem. Suppose matrix* $A = aI; a > 0$ *in the coordination control law (20) satisfies the constraint*

$$a^2 > \frac{1}{2}(\frac{c_2}{c_1} - 1)\max_i \kappa_i \tag{23}$$

where $\kappa_i = |J_i|$ *is the cardinality of* J_i *(the index set of the neighbors of vertex i in Graph* $\mathcal{G}$*) and* c_1 *and* c_2 *are as defined in (15). Then, given any initial state defined by* $X_{pi}(0)$; $1 \le i \le n$ *and* $X_c(0)$*, the resulting trajectories* $X_{pi}(t)$ *and* $X_c(t)$ *are driven asymptotically to* 0.

Proof. See the Appendix.

Notice how the two subsystems are connected via d and v. Section 2 showed, under some mild technical assumptions, that $X_{pi} = \mathbf{0}$ is a globally asymptotically stable equilibrium of each path following subsystem. In particular, it was required that the speed $v_i(t)$ be uniformly continuous and that $\lim_{t\to 0} v_i(t) \neq 0$. Under these conditions, the disturbance-like term d_i that appears at the coordination level was shown to vanish asymptotically to zero *if* the speed

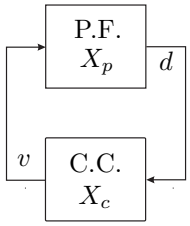

Figure 8. Overall closed-loop system consisting of the path following and coordination control subsystems

v_i is bounded, thus making the states of the coordination system tend asymptotically to zero. It follows from these considerations that X_{pi} and X_c in Figure 8 tend asymptotically to zero if the speed v satisfies the three technical conditions stated above. This is formally shown in the proof of the above proposition.

5. Time-Varying Pattern Tracking

In Section 3 we showed, with the help of simple motivating examples, how the problem of coordinated path following can be essentially reduced to that of "aligning" the coordination states ξ_i asymptotically, that is, making $\xi_i - \xi_j \to 0$ for all i and j as $t \to \infty$. In that section, it was also shown how the coordination ξ_i state of each vehicle yields a re-parametrization of its assigned path as a function of path length s_i, that is, $\xi_i = \xi_i(s_i)$. Using this set-up, formation patterns (compatible with the paths being followed) are obtained by proper choice of the parametrization functions $\xi_i(s)$, which must be computed in advance. In the case of complex but fixed formation patterns that are path-dependent, the re-parametrization can be done but may assume a complicated form. This problem is further aggravated in the case of desired formation patterns that are explicit functions of time, because in this case the above re-parametrization is simply non-existent. This section offers a methodology for time-varying pattern tracking that is simple to implement and overcomes the above problems. The rationale behind the methodology can be explained by referring to the simple case of a number of vehicles doing coordinated path following along parallel straight lines. With $\xi_i = s_i$ and the methods proposed so far, coordination is achieved when the vehicles assume an in-line formation pattern, which will henceforth be called the *baseline pattern* or configuration. Now, it is easy to go from the baseline configuration to a more complex, possibly time-varying formation, by introducing appropriate offsets in the desired positions of the vehicles with respect to the position of a fictitious Leader or with respect to the average point of the formation. We take the latter approach and formalize it as follows. Recall the coordination dynamics

$$\begin{aligned} \dot{\eta} &= u \\ \dot{\xi} &= C\eta + v_{\mathcal{L}}\mathbf{1} + d \end{aligned} \tag{24}$$

and assume as before, at this stage, that $d = \mathbf{0}$. Define α (the *average point of the formation*) and δ (the offset of the vehicles with respect to α) as

$$\alpha = \tfrac{1}{n}\mathbf{1}^T\xi \tag{25}$$

and

$$\delta \quad = \xi - \alpha \mathbf{1}, \tag{26}$$

respectively and notice that $\mathbf{1}^T\delta = 0$. Define now the (pattern-induced) reference vector $h(t)$ with respect to α, which satisfies necessarily the relation $\mathbf{1}^T h(t) = 0$. Then, the problem of time-varying pattern tracking is reduced to that of making $(\delta - h) \to \mathbf{0}$ as $t \to \infty$.

With the change of variables

$$\begin{array}{rcl} \mu & = & \eta - C^{-1}\dot{h} \\ \theta & = & Y M_1^T(\xi - h) \\ u_0 & = & \frac{d}{dt}(C^{-1}\dot{h}), \end{array} \tag{27}$$

the dynamics of (μ, θ) are given by

$$\begin{array}{rcl} \dot{\mu} & = & u - u_0 \\ \dot{\theta} & = & Y M_1^T C \mu \end{array} \tag{28}$$

The methodology used in the last section can now be exploited to show that the coordination control law $u = u_0 - (A^{-1}M_1Y^2M_1^T + A)C\mu - B\mathrm{sat}(\mu + A^{-1}M_1Y\theta)$ or, equivalently (in the original state-space) the control law

$$u = \frac{d}{dt}(C^{-1}\dot{h}) - (A^{-1}L + A)(C\eta - \dot{h}) - B\mathrm{sat}(\eta - C^{-1}\dot{h} + A^{-1}L(\xi - h)) \tag{29}$$

renders the origin of the closed-loop system uniformly globally asymptotically stable (UGAS). Therefore, $M_1^T(\xi - h) \to \mathbf{0}$ and using the fact that $M_1^T\mathbf{1} = \mathbf{0}$ this implies that $M_1^T(\delta - h) \to \mathbf{0}$. Because $\mathbf{1}^T\delta = 0$ and $\mathbf{1}^T h = 0$, that is, $\delta - h$ is normal to the null space of M_1^T, we conclude that $(\delta - h) \to \mathbf{0}$ as required. In the exposition above, it was implicitly assumed that the reference $h(t)$ is sufficiently smooth in order for its derivatives to exist. □

The above control law can be written in decentralized form as

$$u_i = \frac{d}{dt}(R_i\dot{h}_i) - a_i(\frac{1}{R_i}\eta_i - \dot{h}_i) - \frac{1}{a_i}\sum_{j\in J_i}(\frac{1}{R_i}\eta_i - \dot{h}_i - \frac{1}{R_j}\eta_j + \dot{h}_j)$$

$$-b_i\,\mathrm{sat}(\eta_i - R_i\dot{h}_i + \frac{1}{a_i}\sum_{j\in J_i}(\xi_i - h_i - \xi_j + h_j)).$$

Notice that vehicle i needs to know the difference $\xi_j - h_j$ between the coordination variable ξ_j and reference h_j of vehicle j (but not the coordination state ξ_j itself), together with $\frac{1}{R_j}\eta_j - \dot{h}_j$.

6. Simulations

This section contains the results of simulations that illustrate the performance obtained with the coordinated path following control laws developed in the paper. Figures 9 and 10 illustrate the situation where 3 wheeled robots are required to follow paths that consist of parallel straight lines and nested arcs of circumferences (C piecewise constant). Figure 9 corresponds to the case of an in-line formation pattern. Figure 10 shows the case where the vehicles are required to

keep a triangular formation pattern with constant pattern $h^T = [-0.25, +0.5, -0.25]$. In both simulations, vehicle 1 is allowed to communicate with vehicles 2 and 3, but the last two do not communicate between themselves directly. The reference speed $v_{\mathcal{L}}$ was set to $v_{\mathcal{L}} = 0.1$ [s^{-1}]. Notice how the vehicles adjust their speeds to meet the formation requirements and the path following errors decay to 0. In the in-line formation case (Figure 9), the coordination errors $\xi_{12} = \xi_1 - \xi_2$ and $\xi_{13} = \xi_1 - \xi_3$ converge to zero. In the triangle formation case (Figure 10), $\xi_{12} \to -0.75$ and $\xi_{13} \to 0$ as desired.

Figure 11 illustrates a different kind of coordinated maneuver in the $x - y$ plane: one robot is required to follow the $x-$axis, while the other must follow a sinusoidal path as the two maintain an in-line formation along the $y-$axis. In this case, C is time varying. Notice in Figure 11(b) how vehicle 1 adjusts its speed along the path so as to achieve coordination. As seen in sub-Figures 11(c) and 11(d), the vehicles converge to the assigned paths and drive the error between their $x-$coordinates to 0.

7. Conclusions and suggestions for further research

The paper formulated and presented a solution to the problem of steering a fleet of wheeled robots along a set of given spatial paths, while keeping a desired inter-vehicle formation pattern. The solution adopted for coordinated path following builds on Lyapunov based techniques and addresses explicitly the constraints imposed by the topology of the inter-vehicle communications network. With this set-up, path following (in space) and inter-vehicle coordination (in time) are essentially decoupled. Path following for each vehicle amounts to reducing a conveniently defined error variable to zero. Vehicle coordination is achieved by adjusting the speed of each of the vehicles along its path, according to information on the position of the other vehicles, as determined by the communications topology adopted. The methodology proposed led to a decentralized control law whereby the exchange of data among the vehicles is kept at a minimum. Simulations illustrated the efficacy of the solution proposed. Further work is required to extend the methodology proposed to air and underwater vehicles. Namely, by addressing the problems of robustness against temporary communication failures.

Appendix

Proof of Proposition 1 - Path Following. The key ideas used in the proof borrow from the work of (Soeanto *et al.*, 2003) and (Kaminer *et al.*, 2005), to which the reader is referred for details. Notice that we assumed the speed v of the robot is controlled independently and therefore v is viewed as an exogenous variable that does not tend to 0 as $t \to \infty$. Consider the Lyapunov function candidate

$$V = \frac{1}{2}x_e^2 + \frac{1}{2}y_e^2 + \frac{1}{2}(\psi_e - \sigma)^2 + \frac{1}{2}(r - \phi)^2 \tag{30}$$

which is positive definite and radially unbounded. With N and $\dot{s}$ as in (4) and (5), respectively the time derivative of V along the trajectories of the vehicle with kinematics described in (1) and dynamics $\dot{r} = N$ yields

$$\dot{V} = -k_3 x_e^2 - k_1(\psi_e - \sigma)^2 - k_2|v(t)|\frac{y_e^2}{|y_e| + \epsilon_0} - k_4(r - \phi)^2, \tag{31}$$

which is negative semidefinite (notice that $v(t)$ can go through 0). Define $X_p = (x_e, y_e, \psi_e)^T$. Then, $X_p = \mathbf{0}$ is a stable equilibrium point. Since $||X_p(t)|| < r$, for some $r > 0$, for all $t \geq t_0$ and the vector field in (1) is locally Lipschitz in X_p uniformly in t, we conclude that $X_p(t)$ is uniformly continuous in t on $[t_0, \infty)$. To conclude asymptotic stability start by noticing that because $V(t, X_p(t))$ is nonincreasing and bounded from below by zero, it converges to a limit as $t \to \infty$. From

$$-\int_{t_0}^{t} \dot{V}(\tau, X_p(\tau))d\tau = V(t_0, X_p(t_0)) - V(t, X_p(t)), \tag{32}$$

it follows that $\lim_{t\to\infty} \int_{t_0}^{t} \dot{V}(\tau, X_p(\tau))d\tau$ exists and is finite. Because $X_p(t)$ and $v(t)$ are uniformly continuous, so is $\dot{V}(t, X_p(t))$. A straightforward application of Barbalat's lemma (Khalil, 2002) allows for the conclusion that $\lim_{t\to\infty} \dot{V}(t, X_p(t)) = 0$. Therefore, from (31), x_e, $(\psi_e - \sigma)$, $(r - \phi)$ and $v(t)y_e^2$ vanish as $t \to \infty$. Moreover, since V is bounded below by zero and nonincreasing, we can conclude that $\lim_{t\to\infty} y_e = y_{e,lim}$. Because $\lim_{t\to\infty} v(t) \neq 0$ and $v(t)y_{e,lim}^2$ vanishes, $y_{e,lim} = 0$. As a consequence, the origin $X_p = \mathbf{0}$ is globally attractive and thus globally asymptotically stable.□

Remark 2. Suppose $|v(t)|$ has a positive lower bound, that is $\inf_t |v(t)| = v_m > 0$ for all $t \geq t_0$. Then, for $|y_e(t)| < c$ (where c is an arbitrary constant) one obtains that $\dot{V} \leq -\lambda V$ for $\lambda = \min(k_3, k_1, k_4, \frac{k_2 v_m}{c+\epsilon_0})$. It follows that all states $X_p(t_0)$, such that $V(t_0, X_p(t_0)) < c^2/2; t_0 \geq 0$, decay to 0 exponentially with rate λ.

Remark 3. It is interesting to see what happens when the basic assumption that the speed v should not tend to 0 as $t \to \infty$ is violated. To do this, it is sufficient to examine the situation where $v = 0$ for all $t \geq t_0$, that is, when the vehicle is stopped. In this case $\dot{V}$ is still negative semidefinite and the origin is stable. Again, using Barbalat's lemma it is easily seen that x_e converges to zero while the remaining states are attracted to constant values. In particular, the vehicle orientation tends to an angle that is a function of the steady value of y_e. This property shows that the path following algorithm degrades gracefully when the vehicle comes to a stop.

Proof of Proposition 2 - Coordination. We start by introducing formally the *graph-induced coordination error* as

$$\theta = Y M_1^T \xi, \tag{33}$$

with M_1 and Y as defined in Section 3. Recall that $\text{Rank} M_1 = n - 1$, $M_1^T \mathbf{1} = \mathbf{0}$, $M_1^T M_1$ is invertible, and $Y > 0$. From these relations, $\theta = \mathbf{0}$ is equivalent to $\xi_i = \xi_j, \forall i, j$. Consequently, if θ is driven to zero asymptotically, so are the coordination errors $\xi_i - \xi_j$ and the problem of coordinated path following is solved. This justifies the choice of the above error vector.

With the control law (20), the dynamics of the coordination system (14) can be written in terms of η and θ as

$$\begin{array}{rcl} \dot{\eta} & = & -(A^{-1} M_1 Y^2 M_1^T + A) C\eta - B\,\text{sat}(\eta + A^{-1} M_1 Y \theta), \\ \dot{\theta} & = & Y M_1^T C\eta + Y M_1^T d. \end{array} \tag{34}$$

in which we used the fact that $M_1^T v_{\mathcal{L}} \mathbf{1} = \mathbf{0}$. Let

$$z = \eta + A^{-1} M_1 Y \theta$$

and consider the candidate Lyapunov function

$$V = \frac{1}{2}\theta^T\theta + \frac{1}{2}z^T z.$$

Clearly, V is positive definite and radially unbounded on (η, θ). Computing the derivative of V along the solutions of (34) with $d = \mathbf{0}$ yields

$$\dot{V} = -\eta^T AC\eta - z^T B\text{sat}(z).$$

which is negative definite with respect to $(\eta^T, z^T)^T = \mathbf{0}$, or equivalently with respect to $(\eta^T, \theta^T)^T = \mathbf{0}$, since M_1 is full rank and $Y > 0$. Therefore the origin is a UGAS equilibrium point of (34). □

Proof of Proposition 3 - Path Following and Coordination Interconnection.

Define $V_\eta = \eta^T\eta$ and compute its derivative along the solutions of the coordination subsystem (34) to obtain

$$\dot{V}_\eta \quad = -\eta^T CQC\eta - 2\eta^T B\,\text{sat}(\eta + A^{-1}M_1 Y\theta)$$

where $Q = C^{-1}A^{-1}L + LC^{-1}A^{-1} + 2C^{-1}A$. From Lemma 4 in the Appendix, and because $C(t)$ is diagonal and has a positive uniform lower bound c_1, it follows from condition (23) that there exists $\bar{\gamma} = \gamma c_1^2 > 0$ such that $\eta^T CQC\eta \geq \bar{\gamma}||\eta||^2$ and therefore

$$\dot{V}_\eta \leq -\bar{\gamma}||\eta||^2 + 2b_m x_m\sqrt{n}||\eta||,$$

where $b_m = \max_i b_i; i = 1, 2, .., n$. Clearly, $\dot{V}_\eta$ is negative if $||\eta|| > 2b_m x_m\sqrt{n}/\bar{\gamma}$. Therefore, η is uniformly ultimately bounded and so is $v(t) = \eta + v_{\mathcal{L}}C^{-1}\mathbf{1}$. See (Khalil, 2002) for the definition of ultimate boundedness, together with related results of interest. From the form of the closed-loop dynamics (34) it follows that $\dot{\eta}$ is bounded and therefore $\dot{v}$ is also bounded. As a consequence, $v(t)$ is uniformly continuous.

It is now necessary to show that $\lim_{t\to\infty} v_i(t) \neq 0$ for all i. Assume by contradiction that $\exists j$ such that $v_j(t) = 0$ for all $t > t_0 \geq 0$ and $\lim_{t\to\infty} v_i(t) \neq 0\ \forall i \neq j$ (the analysis for the case where v_j tends to 0 but is not identically 0 after a certain finite time can be done identically). Recall from Remark 3 that all x_{ei}'s converge to zero as $t \to \infty$ *even if* $v_i(t)$ tends to 0. Thus, $d_j = \frac{1}{R_j}[(\cos\psi_{ej} - 1)v_j + k_3 x_{ej}]_{|v_j=0}$ is also bounded and tends to zero. Furthermore, according to Proposition 1, the states $X_{pi}\ \forall i \neq j$ are bounded and converge to zero and so do the d_i's $\forall i \neq j$. Since η and d are bounded, so is $\dot{\theta}$. Therefore θ is bounded in any bounded interval of time. It is easy to check that (34) is small-signal L_∞ stable with d as an input, that is $\exists r > 0$ such that if $||d|| < r$ the states remain bounded. Because $||d|| \to 0$, as $t \to \infty$, then $\exists T > 0 : \forall t > T, ||d(t)|| < r$. Therefore the states remain bounded and decay to zero as $d \to 0$, namely the coordination states X_c vanish asymptotically. Thus, $\eta = v - v_{\mathcal{L}}C^{-1}\mathbf{1}$ and in particular $\eta_j = v_j - R_j v_{\mathcal{L}}$ converge to 0, which contradicts the assumption that $v_j = 0$ because $v_{\mathcal{L}} \neq 0$ and R_j is positive definite. □

Remark 4. The behavior of the signals described above is clearly seen in the simulations: the coordination errors θ increase initially while the vehicles are far from the paths and d is large, and then decay to zero as the vehicles approach the paths and time grows.

Lemma 4. Let $\mathcal{G}$ be a connected graph with Laplacian L of dimension $n \times n$ and let $C(t) = \text{diag}[c_{ii}]_{n\times n}$ be a diagonal matrix satisfying $c_1 I \leq C(t) \leq c_2 I$; $c_1 > 0$. Define

$$Q(t) = C^{-1}(t)A^{-1}L + LC^{-1}(t)A^{-1} + 2C(t)^{-1}A,$$

where $A = aI$. Suppose

$$a^2 > \frac{1}{2} \max_i \kappa_i \, (\frac{c_2}{c_1} - 1) \tag{35}$$

where $\kappa_i = |J_i|$ is the cardinality of J_i, that is, the index set of the neighbors of vertex i in Graph $\mathcal{G}$. Then, there exists $\gamma > 0$ such that $||Q(t)|| > \gamma$ for all $t \geq 0$.

Proof. L has the property that all its diagonal elements are positive and the off diagonals are non-positive. Because A and C are diagonal, Q inherits that property. This, together with Geršgorin's theorem (Horn and Johnson, 1985) imply that if

$$\sum_{j=1}^{n} q_{ij}(t) > \gamma, \ \forall i \tag{36}$$

for some $\gamma > 0$, then $\lambda_{min}(Q(t)) > \gamma$ for all t, equivalently $Q\mathbf{1} > \gamma\mathbf{1}$, where the inequality should be interpreted element by element. Because $L\mathbf{1} = \mathbf{0}$, the above condition degenerates to

$$L[1/c_{ii}a]_{n\times 1} + [2a/c_{ii}]_{n\times 1} > \gamma\mathbf{1}$$

or, using the properties of L, $2a/c_{ii} + \sum_{j\in J_i}(1/c_{ii}a - 1/c_{jj}a) > \gamma$ for all i. Therefore, (36) is satisfied if

$$2a^2 > \kappa_i(\frac{c_2}{c_1} - 1) + \gamma, \ \forall i$$

which is equivalent to (35) because γ can be taken arbitrarily small. □

REFERENCES

Balakrishnan, R. and Ranganathan, K. (2000). *A Textbook of Graph Theory*, Springer.

Beard, R., Lawton, J., and Hadaegh, F. (1999). A coordination architecture for spacecraft formation control. *IEEE Trans. Contr. Syst. Technol.*, vol. 9, pp. 777 - 790.

Biggs, N. (1993). *Algebraic Graph Theory*. Second Edition. Cambridge University Press

Desai, J., Otrowski, J., and Kumar, V (1998). Controlling formations of multiple robots. *Proc. IEEE International Conference on Robotics and Automation (ICRA98)*, pp. 2864-2869.

Encarnação, P., Pascoal, A., and Arcak, M. (2000). Path following for marine vehicles in the presence of unknown currents. *Proc.* 6^{th} *IFAC Symposium on Robot Control (SYROCO'2000)*, Vienna, Austria.

Encarnação, P. and Pascoal, A. (2000). 3D Path following for autonomous underwater vehicles. *Proc. IEEE Conf. Decision and Control (CDC'2000)*, Sydney, Australia.

Encarnação, P., and Pascoal, A. (2001). Combined trajectory tracking and path following: an application to the coordinated control of marine craft. *IEEE Conf. Decision and Control (CDC'2001)*, Orlando, Florida.

Fax, A. and Murray, R. (2002a). Information Flow and Cooperative Control of Vehicle Formations. *Proc. 2002 IFAC World Congress*, Barcelona, Spain.

Fax, A. and Murray, R. (2002b). Graph Laplacians and Stabilization of Vehicle Formations. *Proc. 2002 IFAC World Congress*, Barcelona, Spain.

Fossen, T. (1994). *Guidance and Control of Ocean Vehicles*. John Willey & Sons, Inc., New York.

Ghabcheloo, R., Pascoal, A., Silvestre, C., and Kaminer, I. (2004a). Coordinated Path Following Control of Multiple Wheeled Robots. *Proc. 5th IFAC Symposium on Intelligent Autonomous Vehicles*, July 5-7, 2004. Lisbon, Portugal.

Ghabcheloo, R., Pascoal, A., and Silvestre, C. (2004b).*Coordinated Path Following Control using Linearization Techniques*. Internal Report CPF01, Institute for Systems and Robotics, Jan. 2004.

Ghabcheloo, R., Pascoal, A., and Silvestre, C. (2004c).*Coordinated Path Following Control using Nonlinear Techniques*. Internal Report CPF02, Institute for Systems and Robotics, Nov. 2004.

Ghabcheloo, R., Pascoal, A., and Silvestre, C. (2004d).*Nonlinear Coordinated Path Following Control of Multiple Wheeled Robots with Communication Constraints. International Conference on Advanced Robotics (ICAR)*, July 18-20, 2005. Seatle, USA.

Giuletti, F., Pollini, L., and Innocenti, M. (2000). Autonomous formation flight. *IEEE Control Systems Magazine*, vol. 20, pp. 34 - 44.

Godsil, C. and Royle, G. (2001). *Algebraic Graph Theory*. Graduated Texts in Mathematics, Springer-Verlag New York, Inc.

Horn R. A., and Johnson C. R. (1985). *Matrix Analysis*. Cambridge Univ. Press.

Kaminer, I., Pascoal, A., Khargonekar, P., and Coleman, E. (1995). A velocity algorithm for the implementation of gain-scheduled controllers. *Automatica*, Vol. 31. No.1, pp. 1185 - 1191.

Kaminer, I., Pascoal, A., Hallberg, E., and Silvestre, C. (1998). Trajectory Tracking for Autonomous Vehicles: An Integrated Approach to Guidance and Control. *Journal Of Guidance, Control, and Dynamics*, Vol. 21, No.1, pp. 29-38.

Kaminer, I., Pascoal, A. and Yakimenko, O. (2005). Nonlinear Path Following Control of Fully Actuated Marine Vehicles with Parameter Uncertainty, *16th IFAC World Congress*, Prague, Czech Republic.

Khalil, H. K. (2002). *Nonlinear Systems*. Third Edition, Prentice Hall.

Lapierre, L., Soetanto, D., and Pascoal, A. (2003a). Coordinated motion control of marine robots. *Proc. 6th IFAC Conference on Manoeuvering and Control of Marine Craft (MCMC2003)*, Girona, Spain.

Lapierre, L., Soetanto, D. and Pascoal, A. (2003b). Nonlinear path following control of autonomous underwater vehicles. *Proc. 1st IFAC Conference on Guidance and Control of Underwater Vehicles (GCUV'03)*, Newport, South Wales, UK.

Mesbahi, M. and Hadaegh, F.Y.(2001). Formation flying control of multiple spacecraft via graphs, matrix inequalities, and switching. *Journal of Guidance, Control and Dynamics*, Vol. 24, No. 2, March-April 2001, pp. 369-377.

Micaelli, A. and Samson, C. (1993). Trajectory - tracking for unicycle - type and two - steering - wheels mobile robots. *Technical Report No. 2097*. INRIA, Sophia-Antipolis, France.

Ögren, P., Egerstedt, M., and Hu, X. (2002). A control lyapunov function approach to multiagent coordination. *IEEE Trans. on Robotics and Automation*, Vol. 18, Issue 5, Oct. 2002 pp. 847-851

Olfati Saber, R. and Murray, R. M. (2003). Agreement Problems in Networks with Directed Graphs and Switching Topology. *Conference on Decision and Control (CDC2003)*, Hawaii, USA.

Pascoal, A. et al. (2000). Robotic ocean vehicles for marine science applications: the european ASIMOV Project. *Proc. OCEANS'2000 MTS/IEEE*, Rhode Island, Providence, USA.

Pratcher, M., D'Azzo, J., and Proud, A. (2001). Tight formation control. *Journal of Guidance, Control and Dynamics*, Vol. 24, No. 2, March-April 2001, pp. 246-254.

Queiroz, M., Kapila, V., and Yan, Q. (2000). Adaptive nonlinear control of multiple spacecraft formation flying. *Journal of Guidance, Control and Dynamics*, Vol. 23, No.3, May-June 2000, pp. 385-390.

Rouche, N., Habets, P. and Laloy, M. (1993). *Stability theory by Liapunov's direct method*. Springer-Verlag New York, Inc.

Sivestre, C. (2000). Multi-Objective Optimization Theory with Applications to the Integrated Design of Controllers Plants for Autonomous Vehicles. PhD thesis (in English). Instituto Superior Técnico, Lisbon, Portugal.

Silvestre, C. and Pascoal, A. (2002). On the Design of Gain-Scheduled Trajectory Tracking Controllers. *International Journal of Robust and Nonlinear Control*, 12:797-839.

Skjetne, R., Moi, S., and Fossen, T. (2002). Nonlinear formation control of marine craft. *Proc. IEEE Conf. on Decision and Control (CDC2002)*, Las Vegas, NV.

Skjetne, R., Flakstad, I., and Fossen, T. (2003). Formation control by synchronizing multiple maneuvering systems. *Proc. 6th IFAC Conference on Manoeuvering and Control of Marine Craft (MCMC2003)*, Girona, Spain.

Soetanto, D., Lapierre, L., and Pascoal, A. (2003). Adaptive, Non-Singular Path Following, Control of Dynamic Wheeled Robots *Proc. ICAR'03*, Coimbra, Portugal.

Sontag E. D. and Wang, Y.(Sept. 1996). New characterizations of input-to-state stability. *IEEE Trans. on Automatic Control*, Vol.41 Issue 9., pp 1283-1294

Stilwell, D. and Bishop, B. (2000). Platoons of underwater vehicles. *IEEE Control Systems Magazine*, December, 2000, pp. 45-52.

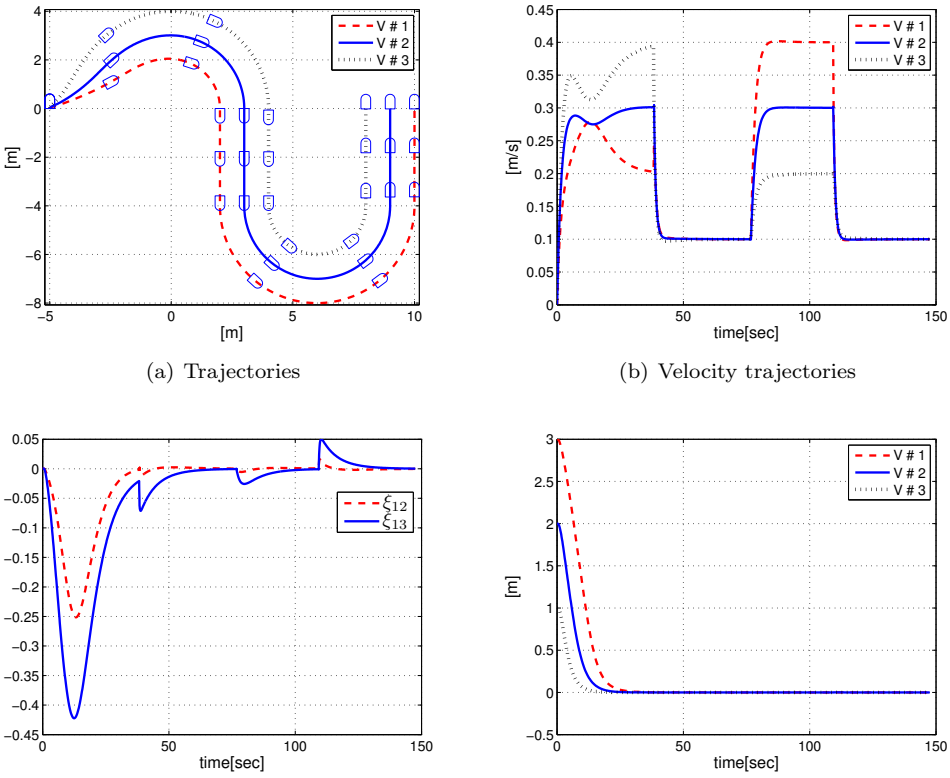

(a) Trajectories

(b) Velocity trajectories

(c) Coordination errors

(d) Path following errors (y_e)

Figure 9. In-line formation, piecewise constant C

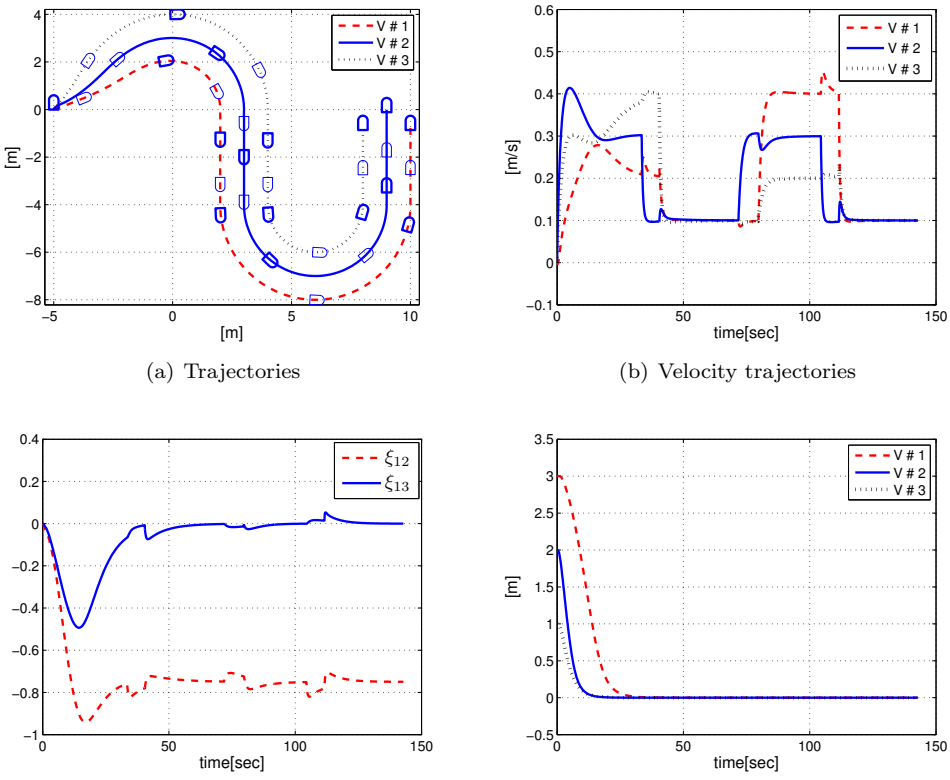

(a) Trajectories

(b) Velocity trajectories

(c) Coordination errors

(d) Path following errors (y_e)

Figure 10. Triangular formation, piecewise constant C

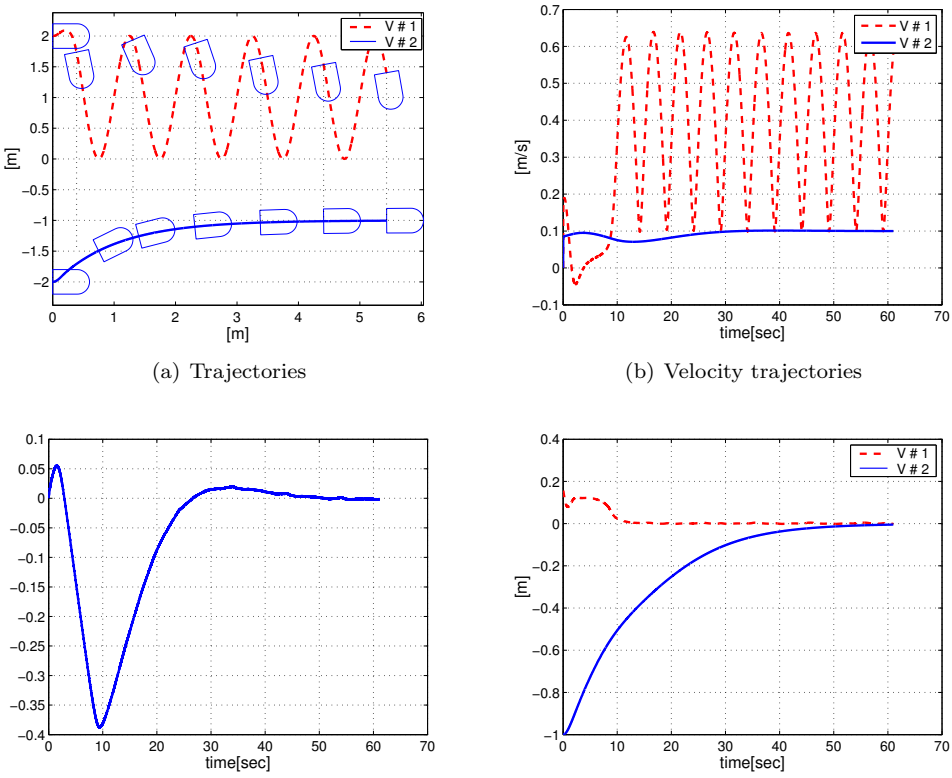

(a) Trajectories

(b) Velocity trajectories

(c) Coordination error

(d) Path following errors (y_e)

Figure 11. Coordination of 2 vehicles, varying C